RUNX2 mutation impairs osteogenic differentiation of dental follicle cells

Yang Liu[a], Xiangyu Sun[a], Xianli Zhang[b], Xiaozhe Wang[a], Chenying Zhang[a,*], Shuguo Zheng[a,*]

[a] *Department of Preventive Dentistry, Peking University School and Hospital of Stomatology, National Engineering Laboratory for Digital and Material Technology of Stomatology, Beijing Key Laboratory of Digital Stomatology, Beijing, PR China*
[b] *Department of Stomatology, Xuanwu Hospital Capital Medical University, Beijing, PR China*

ABSTRACT

Objectives: Cleidocranial dysplasia (CCD), mainly caused by *RUNX2* mutation, is a dominantly inherited skeletal disorder with many dental abnormalities, characterized by delayed permanent tooth eruption. In this study, we explored a novel *RUNX2* mutation and the effect of *RUNX2* mutation on osteogenic differentiation of dental follicle cells (DFCs).
Design: A CCD patient with typical clinical features was involved in this study. Conservation and secondary structural analysis of the *RUNX2* mutation was first performed. Then DFCs that stably expressing wild-type or mutant RUNX2 were established using lentiviruses. Cell Counting Kit 8 (CCK8) assays were performed to test the proliferation of DFCs. Measurement of alkaline phosphatase (ALP) activity, ALP staining, alizarin red staining and determination of osteoblast-specific genes expression were performed to assess osteogenic capacity of DFCs.
Results: A missense mutation (c.674 G > T, p. R225 L) of *RUNX2* gene was identified in the CCD patient. Conservation and secondary structural analysis revealed that the mutation was located in highly conserved Runt domain and altered secondary structure of RUNX2. CCK8 assays showed that mutant RUNX2 increased the proliferation rate of DFCs compared to wild-type RUNX2. ALP activity, ALP staining and alizarin red staining results indicated that mutant RUNX2 decreased the mineralization ability of DFCs. In addition, mutant RUNX2 significantly down-regulated the expression of osteoblast-associated genes.
Conclusions: RUNX2 mutation can reduce the osteogenic capacity of DFCs by inhibiting osteoblast-associated genes and then affecting bone formation, which participates in bone remodeling during tooth eruption. These effects may be partly responsible for the defects in permanent tooth eruption of CCD patients.

1. Introduction

Runt-related transcription factor-2 (*RUNX2*), a member of the *RUNX* family located on chromosome 6p21, is essential for bone and cartilage development and maintenance (Komori et al., 1997; Otto et al., 1997). As a master osteogenic-specific transcription factor, RUNX2 specifically regulates the expression of several genes related to bone and tooth development, including osterix (*OSX*), osteocalcin (*OCN*), bone sialoprotein (*BSP*), osteopontin (*OPN*) and collagen I (*Col I*) (Xu, Li, Hou, & Fang, 2015). RUNX2 was shown to be continuously expressed during intramembranous ossification and endochondral ossification (Bruderer, Richards, Alini, & Stoddart, 2014). In addition, *RUNX2* was also shown to be expressed in dental epithelium, dental papilla and dental follicles during tooth development and eruption (Bronckers, Engelse, Cavender, Gaikwad, & D'Souza, 2001).

RUNX2 mutation is closely associated with cleidocranial dysplasia (CCD; MIM 119600), an inherited autosomal-dominant skeletal disorder with high penetrance and variable expressivity (Lee et al., 1997; Mundlos, 1999; Zhang et al., 2010). The main clinical features of CCD include hypoplasia of clavicles, delayed closure of cranial fontanels and sutures, brachycephalic skull, frontal bossing, and dental anomalies, such as supernumerary teeth, prolonged retention of deciduous teeth, and impaction of permanent teeth (Quack et al., 1999; Zhang et al., 2009). However, the phenotypic spectrum varies dramatically among CCD individuals, from patients with only dental anomalies to individuals with all skeletal CCD features (Quack et al., 1999). The dental abnormalities, especially delayed eruption of permanent teeth, are often mentioned by CCD individuals and regarded as the major cause of reduced quality of life (Yoda, Suda, Kitahara, Komori, & Ohyama, 2004; Zhang et al., 2009).

Tooth eruption is a physiologic process that requires bone resorption and bone formation (Wise, 2009). Resorption of the alveolar bone

---

overlying the tooth crown is indispensable for the formation of the tooth eruption pathway (Wise, Yao, Odgren, & Pan, 2005). In addition, bone formation at the base of the crypt provides the motive force for teeth moving through the eruption pathway (Wise & King, 2008; Wise, 2009). Dental follicles, a loose connective tissue sac surrounding the unerupted tooth, play a critical role in regulating tooth eruption (Liu & Wise, 2007). Dental follicles were shown to regulate the required osteoclastogenesis and osteogenesis by producing molecules at critical times during tooth eruption (Wise & King, 2008; Wise, 2009). In addition, dental follicle cells (DFCs) are precursors of alveolar osteoblasts and have been reported to participate in osteogenesis for bone formation during tooth eruption (Pan et al., 2010; Saugspier et al., 2010). Therefore, dental follicles can not only regulate bone remodeling during tooth eruption but also provide osteoblasts for bone formation, which serve as the motive force for tooth eruption.

Previous studies by our research group and others have shown that *RUNX2* mutation could reduce the osteoclast-inductive ability of DFCs, which may restrict bone resorption at the coronal area of unerupted teeth and impede the formation of the tooth eruption pathway (Ge et al., 2015; Wang et al., 2016). However, whether the eruption force was impacted by *RUNX2* mutation is still unknown. To investigate the effect of mutant RUNX2 on osteogenic differentiation of DFCs, we established cells stably expressing wild-type RUNX2 or mutant RUNX2 in DFCs. Then, measurement of alkaline phosphatase (ALP) activity, ALP staining, alizarin red staining and determination of osteoblast-specific gene expression were performed to assess the osteogenic capacity of DFCs.

2. Materials and methods

2.1. Participants

A 12-year-old boy, clinically and genetically diagnosed as CCD, and three unaffected individuals (aged 10–12 years) participated in this study with informed consent. This study was ethically approved by the Ethical Committee of Peking University School and the Hospital of Stomatology (approval No. PKUSSIRB-2012004). In addition, the protocols were carried out in accordance with the relevant guidelines, including any relevant details.

2.2. Mutation analysis

To detect *RUNX2* status in the CCD patient, we extracted DNA from peripheral blood samples of the participants with General AllGen Kit (Cwbiotech, Beijing, China) according to the manufacture's protocol. The exons (0–7) and exon-intron boundaries of *RUNX2* gene was amplified by polymerase chain reaction (PCR), and the PCR products were then sequenced with an ABI 3730 sequencer (Zhang et al., 2017). The mutation was confirmed by at least two independent experiments of nucleotide sequencing.

2.3. Conservation and secondary structural analysis

Conservation analysis of the affected amino acids of RUNX2 among nine species was performed by the library of Homologene database (http://www.ncbi.nlm.nih.gov/homologene). Secondary structure of wild-type and mutant RUNX2 were predicted by PsiPred 3.3 (http://bioinf.cs.ucl.ac.uk/psipred).

2.4. Cell culture

Dental follicle tissues were collected during exposure of impacted maxillary central incisors for orthodontic treatment. Then, the tissues were rinsed by sterile phosphate buffered saline (PBS), cut into approximately 1 mm^3 pieces and digested in collagenase I (Sigma-Aldrich, MO, US) and dispase II (Sigma-Aldrich) for 40 min at 37 ˚C. Cells were

collected by centrifugation at 1000 rpm and cultured in a proliferation medium (PM) containing DMEM (Gibco, NY, USA), 10% fetal bovine serum (Gibco), 100 U/mL penicillin (Gibco) and 100 μg/mL streptomycin (Gibco) in an incubator at 37 ˚C with 5% CO_2. For osteogenic induction, DFCs were cultured in osteogenic induction medium (OM) containing 100 nM/L dexamethasone (Sigma-Aldrich), 10 mM/L β-glycerophosphate (Sigma-Aldrich), and 50 μg/ml L-ascorbic acid (Sigma-Aldrich) in addition to PM.

2.5. Lentivirus construction and establishment of stably transfected DFCs

For generation of wild-type RUNX2 and mutant RUNX2 (c. 674 G > T, p. R225 L) overexpression lentiviruses, wild-type RUNX2 and mutant RUNX2 cDNA were separately subcloned into the pHBLV-CMVIE-ZsGreen-T2A-puro vector with EcoRI and BamHI (NEB, MA, USA). The recombinant vectors and the packaging vectors psPAX2 and pMD2.G were transfected into 293 T cells to produce the lentivirus. The supernatant was harvested, filtered, and concentrated 2 days after transfection. Lentivirus containing a green fluorescent protein (GFP) tag without the target gene was used as a negative control. For establishment of stably expressing human wild-type RUNX2 or mutant RUNX2 in DFCs, lentiviruses (multiplicity of transfection = 100) mixed with 10 μg/ml polybrene (Sigma-Aldrich) were used to transfect DFCs at the second passage. Then, the transfected cells were selected in the presence of 1 μg/ml puromycin (Sigma-Aldrich) for 7 days. Stably transfected DFCs were observed under a fluorescence microscope to determine the ratio of GFP-positive cells, which reflects the transfection efficiency. Real-time PCR and Western blotting were used to detect the expression of RUNX2 in stably transfected DFCs. DFCs transfected with wild-type RUNX2, mutant RUNX2 recombinant lentivirus or GFP control lentivirus were defined as DFCs-WT, DFCs-MT, and DFCs-CON, respectively.

2.6. Cell proliferation assay

Cell proliferation was assessed by Cell Counting Kit 8 (CCK-8, Dojindo, Kumamoto, Japan) assays according to the manufacturer's instructions. Briefly, stably transfected DFCs were seeded in 96-well plates at a cell density of 2×10^3 cells/well in triplicate and cultured in complete medium for 14 days. Every other day, the supernatant was removed, and the DFCs were incubated in complete medium containing 10% CCK-8 regent for 2 h. The optical density at 450 nm was examined by an ELx808 absorbance microplate reader (BioTek, Winooski, VT).

2.7. ALP staining and quantification of ALP activity

DFCs were seeded at a density of 4×10^4 cells/well in 12-well plates. When 80% confluence was reached, the medium was changed to OM and cultured for 7 and 14 days. At the indicated time, ALP staining was performed using an ALP histochemical staining kit (Cwbiotech, Beijing, China) according to the manufacturer's instructions. Briefly, DFCs were rinsed with PBS 3 times and fixed in 95% ice-cold alcohol for 30 min, washed with Millipore-filtered water, and stained with NBT/BCIP solution for 10 min at room temperature. The images of ALP staining were captured by a scanner (HP, CA, USA).

ALP activity was analyzed using an ALP activity assay kit (Jiancheng, Nanjing, China) according to the manufacturer's instructions. The absorbance at 520 nm was measured using a spectrophotometric instrument (PerkinElmer, Waltham Mass, MA). Protein concentration was determined by a BCA kit (Thermo Fisher Scientific, Waltham, MA), which was used to normalize the ALP activity. The ALP activity was calculated relative to that of the control group.

2.8. Alizarin red staining

After induction for 21 days in OM, DFCs were rinsed 3 times with

PBS, fixed in 95% ice-cold alcohol for 30 min, and washed with Millipore-filtered water 3 times. Then, DFCs were incubated with 2% alizarin red (Sigma-Aldrich) for 20 min at room temperature. The images of alizarin red staining were captured by a microscope equipped with a camera (Leica, HE, Germany). For quantification of matrix mineralization, the stained samples were eluted in 100 mM cetylpyridinium chloride (Sigma-Aldrich) for 1 h to solubilize the alizarin red into the solution. Then, the absorbance at 562 nm of the released alizarin red was measured by a spectrophotometric instrument (PerkinElmer). The alizarin red intensity was calculated relative to that of the control group.

2.9. Real-time PCR analysis

Total RNA was extract with TRIzol reagent (Invitrogen, CA, USA) and reverse-transcribed into cDNA with a reverse transcription kit (Thermo Fisher Scientific) according to the manufacturer's protocol. Real-time PCR was conducted using the SYBR Green PCR kit (Roche Applied Science, IN, USA) on an ABI 7500 Real-time PCR System (Applied Biosystems, CA, USA). The relative mRNA expression was normalized to glyceraldehyde phosphate dehydrogenase (GAPDH) and calculated using the $2^{-\Delta\Delta Ct}$ method (Siegling, Lehmann, Platzer, Emmrich, & Volk, 1994). The sequences of the primers used in this study are listed in Table 1.

2.10. Western blotting analysis

Cells were harvested and lysed in RIPA buffer containing proteinase inhibitors. Protein concentration was tested with a BCA kit (Thermo Fisher Scientific). Protein samples were electrophoresed in 10% sodium dodecyl sulfate polyacrylamide gels and transferred to polyvinylidene difluoride membranes (Millipore, MA, USA). After being blocked in 5% skim milk for 1 h, membranes were incubated with primary antibodies against RUNX2 (CST, MA, USA), OSX and Col 1α1 (Abcam, Cambridge, UK) and GAPDH (CST) separately overnight at 4 °C, followed by incubation with HRP-conjugated secondary antibodies for 1 h at room temperature. The immune-reactive bands were detected using an enhanced chemiluminescence blotting kit (Cwbiotech) on an Odyssey infrared imaging system (Odyssey LI-COR Biosciences, Lincoln, NE). The background was subtracted, and the signal of each target band was normalized to that of the GAPDH band.

2.11. Statistical analysis

All the experiments were repeated at least 3 times independently. All data are presented as the mean and standard deviation. Differences between groups were analyzed by one-way analysis of variance, and $P < 0.05$ was considered statistically significant.

3. Result

3.1. Clinical manifestation of the CCD patient and RUNX2 mutation analysis

The patient involved in this study was a familial case with three family members affected in this family (Fig. 1A). The proband showed typical CCD phenotypes, including incomplete fontanelles (Fig. 1B), multiple Wormian bones in the lambdoid and sagittal sutures (Fig. 1C), bilateral aplasia of clavicles (Fig. 1D). Panoramic radiograph of the CCD patient showed retained deciduous teeth, delayed eruption of permanent teeth and absence of the mandibular second premolars (Fig. 1E). The panoramic radiograph of the patient had been shown in the previous papers of our research group (Zhang et al., 2010). In addition, a missense mutation (c. 674 G > T, p. R225 L) in the exon 3 of *RUNX2* was found in this patient (Fig. 1F–G). Conservation analysis revealed that the affected residues in the *RUNX2* gene showed a high level of evolutionary conservation among nine species (Fig. 1G). Secondary structure analysis demonstrated that this missense mutation resulted in changes of the RUNX2 protein structure, and the changes were mainly located in the Runt domain (Fig. 2). Mutation of the highly conserved residues and changes in the secondary structure appeared to impair the function of the RUNX2 protein.

3.2. Overexpression of wild-type RUNX2 and mutant RUNX2 in DFCs

Stable overexpression of wild-type RUNX2 and mutant RUNX2 in DFCs was established as described in the Materials and methods. As the transfected lentiviruses contained a GFP tag, fluorescence analysis was used to detect the transfection efficiency. The results showed that GFP expression was observed in almost all stably transfected DFCs under fluorescence microscopy (Fig. 3A). Real-time PCR analysis showed that RUNX2 mRNA expression was increased more than 10-fold in DFCs transfected with wild-type RUNX2 or mutant RUNX2 compared with the control group ($P < 0.05$) (Fig. 3B). Consistently, the RUNX2 protein level was also significantly increased in the DFCs-WT and DFCs-MT groups compared with the control group ($P < 0.05$) (Fig. 3C). These results indicated that wild-type RUNX2 or mutant RUNX2 was stably overexpressed in DFCs.

3.3. RUNX2 mutation results in increased proliferation of DFCs

To investigate the effect of the *RUNX2* mutation on the proliferation of DFCs, we performed CCK-8 assays. As shown in Fig. 4, the DFCs-WT group exhibited a significantly lower proliferation rate than the DFCs-CON group from day 5 to day 13 ($P < 0.05$), indicating that wild-type RUNX2 could inhibit DFCs proliferation. However, the cell proliferation rate in the DFCs-MT group was higher than that of the DFCs-WT group and the DFCs-CON group from day 5 to day 13 ($P < 0.05$). These results indicate that RUNX2 acts as a negative regulator of DFCs proliferation, while mutant RUNX2 lost this inhibitory effect and could even promote cell proliferation.

3.4. RUNX2 mutation interferes with the mineralization capacity of DFCs

DFCs are multipotent mesenchymal stem cells that can differentiate into osteoblasts, adipocytes, chondrocytes, and neural cells under different *in vitro* conditions. To assess the effect of wild-type and mutant RUNX2 on the osteogenic ability of DFCs, we tested ALP activity, ALP staining and alizarin red staining. ALP staining showed that ALP expression was significantly increased in DFCs-WT but strongly decreased in the DFCs-MT group compared with the DFCs-CON group, and the difference was much clearer after osteogenic induction (Fig. 5A). ALP activity assays further confirmed these results by showing higher ALP activity in DFCs-WT and lower activity in DFCs-MT after osteogenic induction for 7 days or 14 days ($P < 0.05$) (Fig. 5B–C). Alizarin red

Table 1
Primer sequences of selected genes used in real-time PCR.

Genes	Forward primer	Reverse primer
GAPDH	CGACAGTCAGCCGCATCTT	CCAATACGACCAAATCCGTTG
RUNX2	GATGACACTGCCACCTCTGAC	GGGATGAAATGCTTGGGAAC
ALP	GACCTCCTCGGAAGACACTC	TGAAGGGCTTCTTGTCTGTG
OSX	CCTCCTCAGCTCACCTTCTC	GTTGGGAGCCCAAATAGAAA
OCN	AGCAAAGGTGCAGCCTTTGT	GCGCCTGGGTCTCTTCACT
OPN	ATGATGGCCGAGGTGATAGT	ACCATTCAACTCCTCGCTTT
Col 1α1	GAGGGCCAAGACGAAGACATC	CAGATCACGTCATCGCACAAC

Fig. 1. Clinical manifestation of the CCD patient and mutation analysis of the *RUNX2* gene. (A) Pedigree of the CCD patient. The arrow indicates the proband. (B–E) Anteroposterior (B), lateral (C), chest (D) and panoramic (E) radiograph of the CCD patient. (F) Reverse sequencing data of *RUNX2* gene from the CCD patient and normal control. Arrows indicated the mutation site. (G) The location of the *RUNX2* mutation and conservation analysis of RUNX2; the position of the mutated amino acid in our study is indicated using a black box. Q/A, glutamine/alanine rich region; RUNT, runt homology domain; NLS, nuclear-localization signal; PST, proline/serine/threonine rich region.

staining and quantification analysis indicated that the DFCs-WT had the highest formation of mineralized nodules ($P < 0.05$), whereas the mutant RUNX2 significantly decreased the formation of calcified nodules after osteogenic induction for 21 days ($P < 0.05$) (Fig. 6A–B). These results suggest that *RUNX2* mutation has a negative regulatory effect on mineralization of DFCs.

3.5. RUNX2 mutation inhibits osteogenic differentiation of DFCs

The effect of the wild-type RUNX2 and mutant RUNX2 on the expression of osteoblast-specific genes was further investigated. The basal mRNA level of osteogenic markers, such as *ALP, OSX, OCN, Col Iα1,* and *OPN,* was up-regulated 0.4–1.8-fold by the wild-type RUNX2 ($P < 0.05$), while these increasing trends were blocked to different degrees by the mutant RUNX2 ($P < 0.05$) (Fig. 7A–E). After osteogenic induction, these osteogenic-associated genes were all up-regulated in
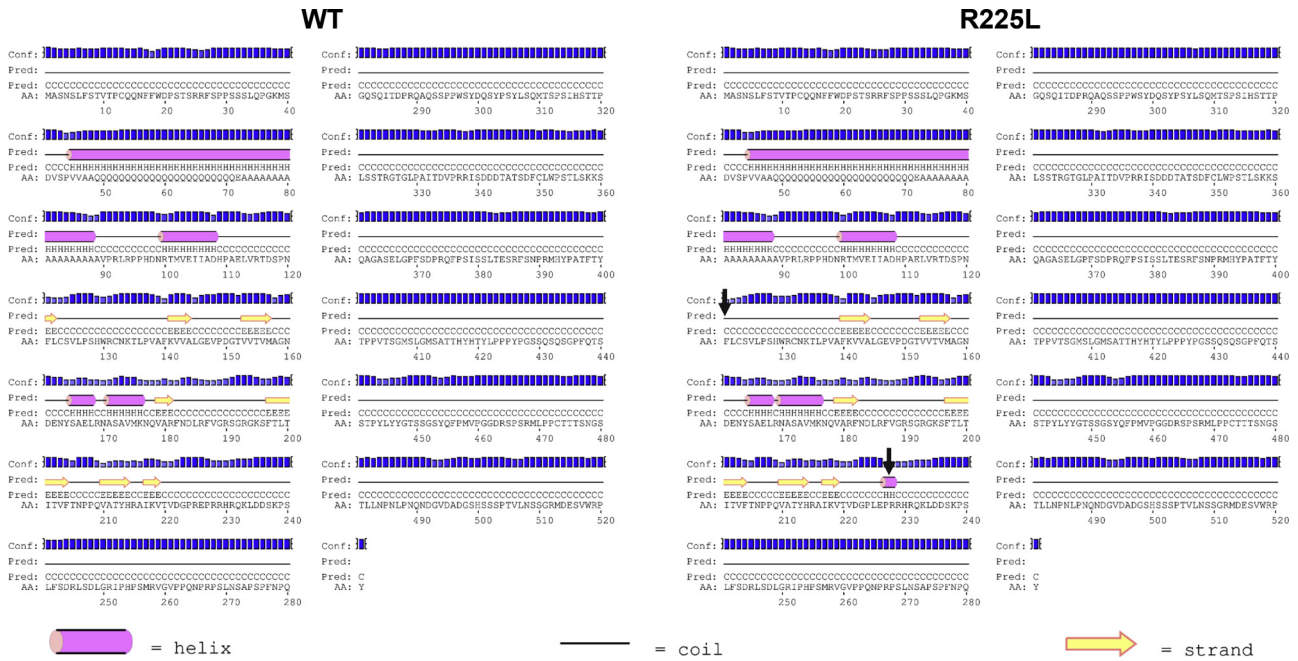
Fig. 2. Secondary structure analysis of the mutated RUNX2. Transformations are marked with black arrows. Pink cylinders represent the helix, yellow arrows represent the strand, and the straight line represents the coil. (For interpretation of the references to colour in this figure legend, the reader is referred to the web version of this article).

the three groups, and the mRNA levels of these genes were substantially increased in DFCs-WT ($P < 0.05$) but evidently decreased in the DFCs-MT group compared with the DFCs-CON group ($P < 0.05$) (Fig. 7A–E). Consistent with the mRNA measurements, Western blotting assays and quantitative analysis of the bands showed that wild-type RUNX2 up-regulated but mutant RUNX2 down-regulated the protein levels of Col Iα1 and OSX compared with the control, especially under osteogenic conditions (Fig. 7F). All these results indicate that mutant RUNX2 can

restrict the expression of osteogenic-associated genes in DFCs.

4. Discussion

In this study, we presented a CCD patient with a missense mutation (c. 674 G > T, p. R225 L) in RUNX2 gene. Our further study demonstrated that the missense *RUNX2* mutation can promote the proliferation and markedly suppress the mineralization capacity of DFCs. In
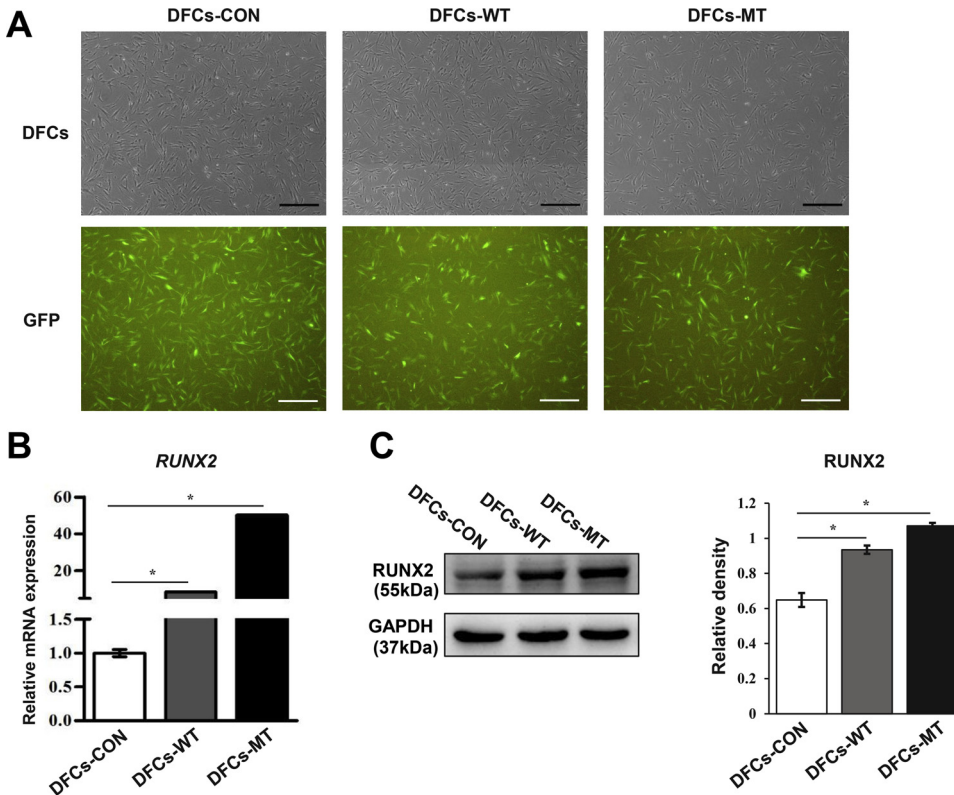
Fig. 3. Overexpression of wild-type and mutant RUNX2 in stably transfected DFCs. DFCs transfected with wild-type RUNX2, mutant RUNX2 recombinant lentivirus or GFP control lentivirus were named as DFCs-WT, DFCs-MT, and DFCs−CON, respectively. (A) GFP expression in stably transfected DFCs. The top row shows normal microscopic views of DFCs, and the bottom row indicates GFP expression, which was photographed by a fluorescence microscope. Scale bar, 500 μm. (B) Quantitative analysis of the mRNA levels of *RUNX2* in stably transfected DFCs. (C) Western blot assays examined the protein level of RUNX2 in DFCs. The histograms show the quantification of band intensities. $^*P < 0.05$.
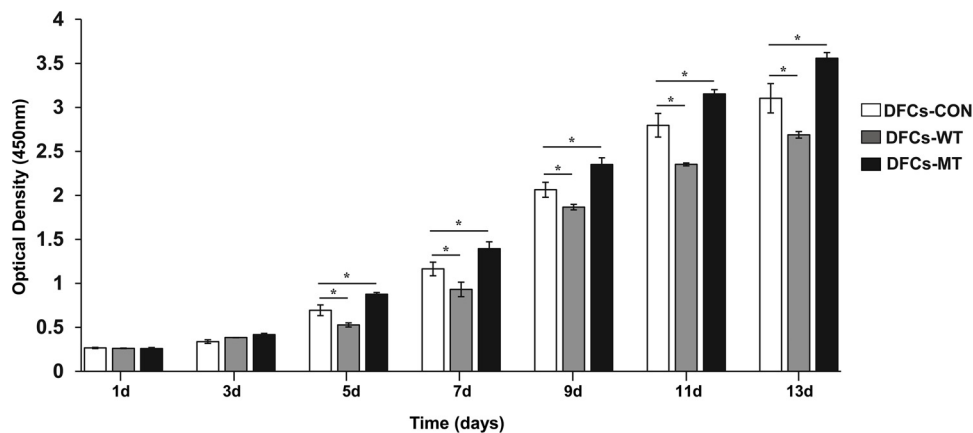
Fig. 4. Effects of mutant *RUNX2* on the proliferation rate of DFCs. DFCs growth rate was measured by CCK-8 assays after the cells were cultured for 2 weeks. [*]$P < 0.05$.

addition, the expression of osteoblast-specific genes, such as *ALP, OSX, OCN, Col Iα1*, and *OPN*, was significantly down-regulated by *RUNX2* mutation. Therefore, the reduced osteogenic ability of DFCs caused by the *RUNX2* mutation may interfere with remodeling of the alveolar bone and may thus be responsible for the delayed eruption of permanent teeth observed in CCD patients.

The RUNX2 protein contains 521 amino acids with several functional domains (Vimalraj, Arumugam, Miranda, & Selvamurugan, 2015). From the N-terminal to the C-terminal, a glutamine-alanine repeat (Q/A) domain, a highly conserved Runt domain and a proline-serine-threonine rich (PST) domain are found on this protein (Bruderer et al., 2014). The Runt domain is mainly responsible for DNA binding to

a specific motif and heterodimerization with core-binding factor subunit beta (CBFβ), a non-DNA-binding subunit (Bruderer et al., 2014). The resulting heterodimers bind to cis-acting elements of RUNX2 target genes and regulate the expression of osteogenic-associated genes, such as osteocalcin and osteopontin. The *RUNX2* mutation involved in this study is located in the Runt domain, and the secondary structural analysis showed that the R225 L mutation altered the secondary structure of the Runt domain. Therefore, we speculate that the mutant RUNX2 led to a defect in heterodimerization and then impaired the transactivation of osteoblast-specific genes.

Because RUNX2 is continuously expressed in differentiated DFCs regardless of osteogenic induction, we explored the effect of *RUNX2*
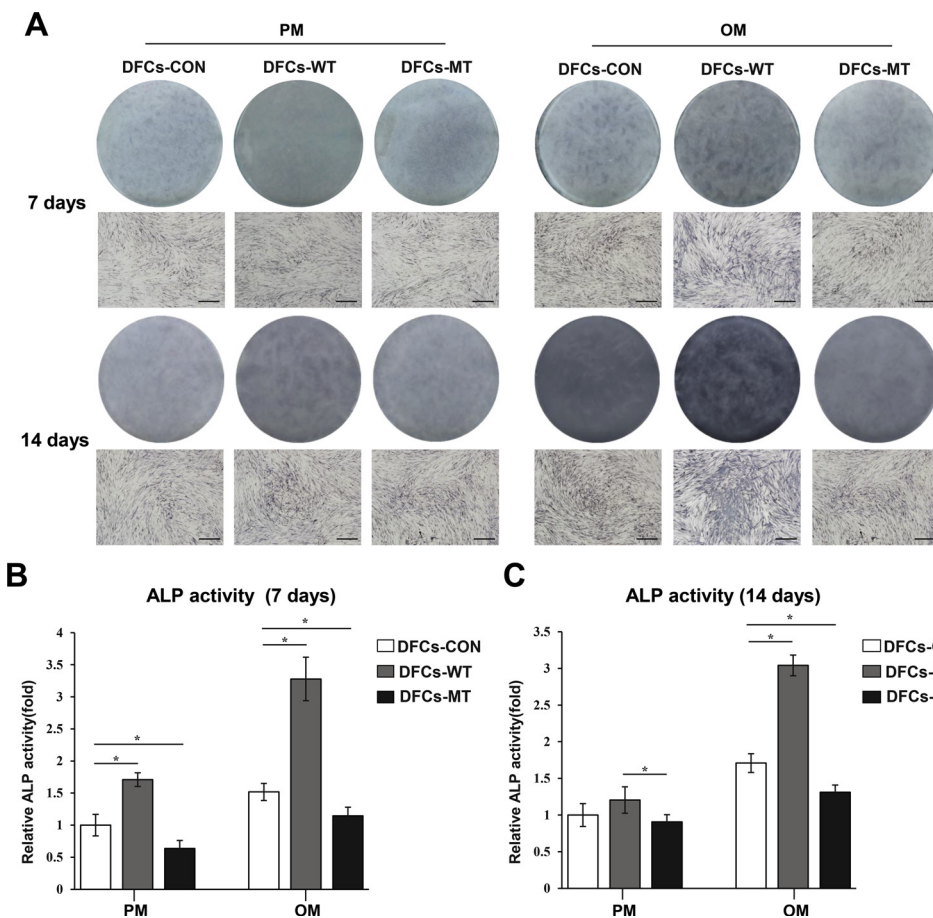
Fig. 5. Mutant *RUNX2* interfered with ALP expression and ALP activity in DFCs. DFCs were cultured in proliferation medium (PM) or osteogenic medium (OM) for 7 days or 14 days. (A) ALP staining of DFCs after induction in PM or OM for 7 days or 14 days. The bottom row indicates microscopic views. Scale bar, 500 μm. (B–C) ALP activity of DFCs was analyzed after incubation in PM or OM for 7 days (B) or 14 days (C). [*]$P < 0.05$.
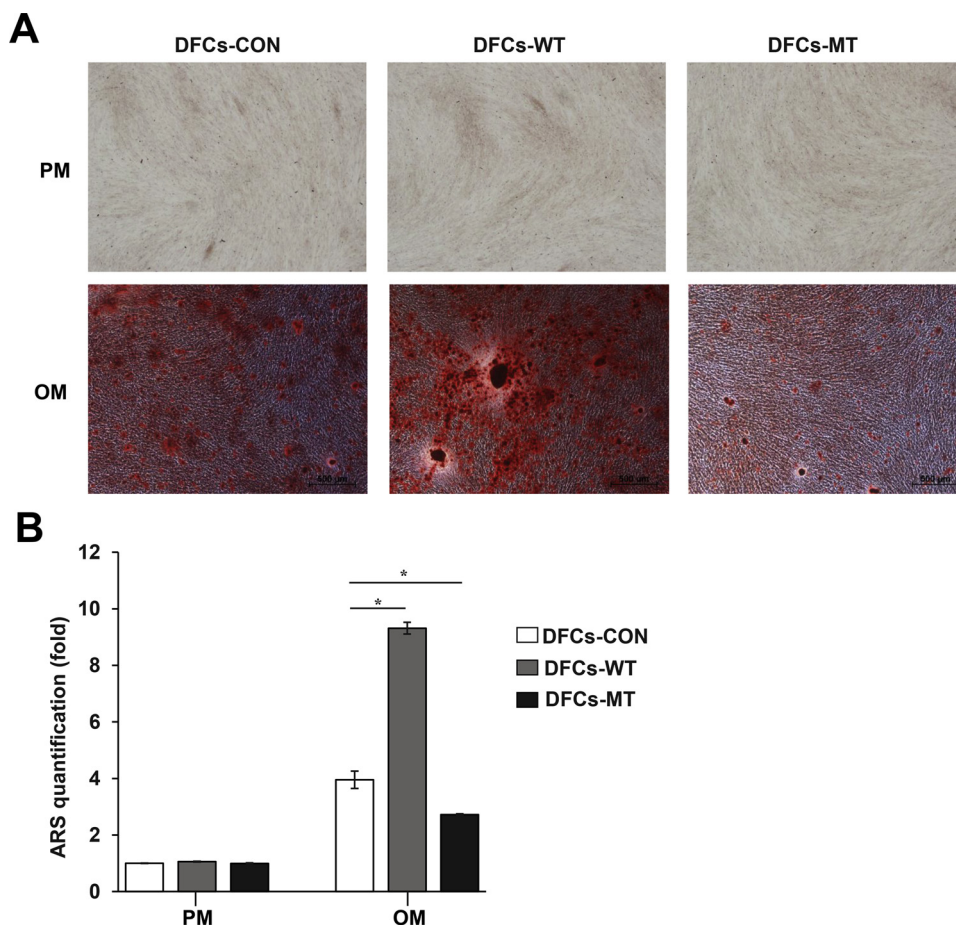
Fig. 6. Mutant *RUNX2* reduced the mineralization ability of DFCs. DFCs were cultured in proliferation medium (PM) or osteogenic medium (OM) for 21 days. (A) Alizarin red staining of mineralized nodules for DFCs. Scale bar, 500 μm. (B) Quantification of alizarin red staining by spectrophotometry. $^*P < 0.05$.
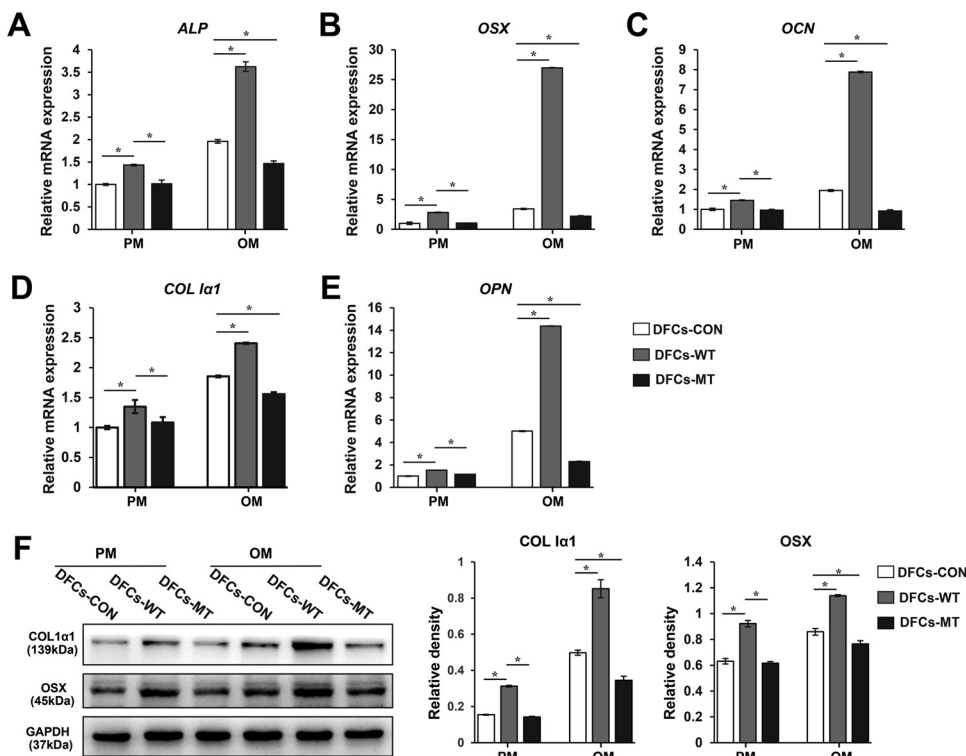
Fig. 7. Mutant RUNX2 down-regulated expression of osteoblast-associated genes in DFCs. (A–E) Quantitative analysis of the mRNA levels of *ALP, OSX, OCN, COLIα1* and *OPN* in DFCs after the cells were cultured in proliferation medium (PM) or osteogenic medium (OM) for 7 days. (F) Western blot assays analyzed the protein level of COL Iα1 and OSX in DFCs after the cells were cultured in PM or OM for 7 days. The histograms show the quantification of band intensities. $^*P < 0.05$.

mutation on the mineralization capacity of DFCs (Morsczeck, 2006; Morsczeck et al., 2009). Our findings showed that the mutant RUNX2 reduced ALP activity and the formation of mineralized nodules. In contrast, wild-type RUNX2 had the opposite effect. Pan et al. reported that overexpression of RUNX2 in DFCs could enhance mineralization of DFCs (Pan et al., 2010). Our results are consistent with their study and further show that the stimulatory function of RUNX2 on the osteogenic differentiation of DFCs was inhibited by the *RUNX2* mutation. The inhibitory effect of *RUNX2* mutation on osteogenic differentiation was also observed in dental pulp cells in a previous study by our research group (Yan et al., 2015).

As an osteoblast-specific transcription factor, RUNX2 plays critical roles in osteogenic differentiation of DFCs by regulating the expression of osteogenic marker genes (Komori, 2017). Our study found that the expression of osteogenic-related genes, including *ALP, OSX, OCN, Col Iα1* and *OPN*, was significantly down-regulated by the *RUNX2* mutation. These findings were consistent with several previous studies showing that the expression of osteogenic marker genes of mesenchymal stem cells isolated from dental pulp, dental follicle and periodontal ligament tissues of CCD patients decreased compared with those of normal individuals (Chen et al., 2014; Yan et al., 2015). These results can be explained by the fact that these genes are regulated by RUNX2 (Komori et al., 1997; Nakashima et al., 2002). In addition, osteoblast-specific element 2 (OSE2), the core-binding site of RUNX2 protein, was present in the promoter region of ALP, OCN, Col Iα1 and OPN (Ducy, 2000). Previous studies of our research group have confirmed that the R225 L mutation impairs the transactivation activity of RUNX2 to OSE2 (Zhang et al., 2009). Therefore, we concluded that *RUNX2* mutation reduced osteogenic differentiation by down-regulating its downstream osteogenic-related genes directly.

Tooth eruption is a localized event that requires chronologically and spatially specific bone remodeling regulated by dental follicles that surround the unerupted tooth (Wise, 2009). Alveolar bone resorption and formation appear not to be coupled during tooth eruption, and resorption occurs in the coronal area of the alveolar bony socket, while bone formation occurs at the base of the socket (Wise & King, 2008). In a scanning electron microscopy (SEM) study of the rat first mandibular molar, trabecular bone (osteogenesis) was observed at the base of the crypt beginning at day 3, and extensive trabecular bone was seen at the base at day 9 (Wise, Yao, & Henk, 2007). An *in vivo* study also showed that if bone formation was inhibited in the local region, an eruption pathway was formed normally due to bone resorption, while the tooth could not erupt because of the lack of eruption force (Bartlett, Zhou, Skobe, Dobeck, & Tryggvason, 2003; Beertsen et al., 2002; Xu et al., 2016). Based on these studies, our research found that *RUNX2* mutation markedly reduced osteogenic differentiation of DFCs, which may result in a deficiency in motive force for unerupted teeth, leading to delayed permanent tooth eruption in CCD patients.

In summary, we confirmed that the CCD-associated *RUNX2* mutation could reduce the ability of primary DFCs to differentiate into osteoblasts and further impair the regulation of bone remodeling during tooth eruption. This may provide valuable explanations and implications for the mechanism of dental abnormalities, namely, delayed eruption of permanent teeth, in CCD patients.

Conflict of interest

None.

Ethical approval

This study was ethically approved by the Ethical Committee of Peking University School and the Hospital of Stomatology (approval No. PKUSSIRB-2012004). All the protocols were carried out in accordance with the relevant guidelines, including any relevant details.

References

Bartlett, J. D., Zhou, Z., Skobe, Z., Dobeck, J. M., & Tryggvason, K. (2003). Delayed tooth eruption in membrane type-1 matrix metalloproteinase deficient mice. *Connective Tissue Research, 44*(Suppl. 1), 300–304.

Beertsen, W., Holmbeck, K., Niehof, A., Bianco, P., Chrysovergis, K., Birkedal-Hansen, H., & Everts, V. (2002). On the role of MT1-MMP, a matrix metalloproteinase essential to collagen remodeling, in murine molar eruption and root growth. *European Journal of Oral Sciences, 110*(6), 445–451.

Bronckers, A. L., Engelse, M. A., Cavender, A., Gaikwad, J., & D'Souza, R. N. (2001). Cell-specific patterns of Cbfa1 mRNA and protein expression in postnatal murine dental tissues. *Mechanisms of Development, 101*(1-2), 255–258.

Bruderer, M., Richards, R. G., Alini, M., & Stoddart, M. J. (2014). Role and regulation of RUNX2 in osteogenesis. *European Cells & Materials, 28*, 269–286.

Chen, P., Wei, D., Xie, B., Ni, J., Xuan, D., & Zhang, J. (2014). Effect and possible mechanism of network between microRNAs and RUNX2 gene on human dental follicle cells. *Journal of Cellular Biochemistry, 115*(2), 340–348.

Ducy, P. (2000). Cbfa1: A molecular switch in osteoblast biology. *Developmental Dynamics, 219*(4), 461–471.

Ge, J., Guo, S., Fu, Y., Zhou, P., Zhang, P., Du, Y., ... Jiang, H. (2015). Dental follicle cells participate in tooth eruption via the RUNX2-MiR-31-SATB2 loop. *Journal of Dental Research, 94*(7), 936–944.

Komori, T. (2017). Roles of Runx2 in skeletal development. *Advances in Experimental Medicine and Biology, 962*, 83–93.

Komori, T., Yagi, H., Nomura, S., Yamaguchi, A., Sasaki, K., Deguchi, K., ... Kishimoto, T. (1997). Targeted disruption of Cbfa1 results in a complete lack of bone formation owing to maturational arrest of osteoblasts. *Cell, 89*(5), 755–764.

Lee, B., Thirunavukkarasu, K., Zhou, L., Pastore, L., Baldini, A., Hecht, J., ... Karsenty, G. (1997). Missense mutations abolishing DNA binding of the osteoblast-specific transcription factor OSF2/CBFA1 in cleidocranial dysplasia. *Nature Genetics, 16*(3), 307–310.

Liu, D., & Wise, G. E. (2007). A DNA microarray analysis of chemokine and receptor genes in the rat dental follicle–role of secreted frizzled-related protein-1 in osteoclastogenesis. *Bone, 41*(2), 266–272.

Morsczeck, C. (2006). Gene expression of runx2, Osterix, c-fos, DLX-3, DLX-5, and MSX-2 in dental follicle cells during osteogenic differentiation in vitro. *Calcified Tissue International, 78*(2), 98–102.

Morsczeck, C., Schmalz, G., Reichert, T. E., Vollner, F., Saugspier, M., Viale-Bouroncle, S., & Driemel, O. (2009). Gene expression profiles of dental follicle cells before and after osteogenic differentiation in vitro. *Clinical Oral Investigations, 13*(4), 383–391.

Mundlos, S. (1999). Cleidocranial dysplasia: Clinical and molecular genetics. *Journal of Medical Genetics, 36*(3), 177–182.

Nakashima, K., Zhou, X., Kunkel, G., Zhang, Z., Deng, J. M., Behringer, R. R., & de Crombrugghe, B. (2002). The novel zinc finger-containing transcription factor osterix is required for osteoblast differentiation and bone formation. *Cell, 108*(1), 17–29.

Otto, F., Thornell, A. P., Crompton, T., Denzel, A., Gilmour, K. C., Rosewell, I. R., ... Owen, M. J. (1997). Cbfa1, a candidate gene for cleidocranial dysplasia syndrome, is essential for osteoblast differentiation and bone development. *Cell, 89*(5), 765–771.

Pan, K., Sun, Q., Zhang, J., Ge, S., Li, S., Zhao, Y., & Yang, P. (2010). Multilineage differentiation of dental follicle cells and the roles of Runx2 over-expression in enhancing osteoblast/cementoblast-related gene expression in dental follicle cells. *Cell Proliferation, 43*(3), 219–228.

Quack, I., Vonderstrass, B., Stock, M., Aylsworth, A. S., Becker, A., Brueton, L., ... Otto, F. (1999). Mutation analysis of core binding factor A1 in patients with cleidocranial dysplasia. *American Journal of Human Genetics, 65*(5), 1268–1278.

Saugspier, M., Felthaus, O., Viale-Bouroncle, S., Driemel, O., Reichert, T. E., Schmalz, G., & Morsczeck, C. (2010). The differentiation and gene expression profile of human dental follicle cells. *Stem Cells and Development, 19*(5), 707–717.

Siegling, A., Lehmann, M., Platzer, C., Emmrich, F., & Volk, H. D. (1994). A novel multispecific competitor fragment for quantitative PCR analysis of cytokine gene expression in rats. *Journal of Immunological Methods, 177*(1-2), 23–28.

Vimalraj, S., Arumugam, B., Miranda, P. J., & Selvamurugan, N. (2015). Runx2: Structure, function, and phosphorylation in osteoblast differentiation. *International Journal of Biological Macromolecules, 78*, 202–208.

Wang, X. Z., Sun, X. Y., Zhang, C. Y., Yang, X., Yan, W. J., Ge, L. H., & Zheng, S. G. (2016). RUNX2 mutation impairs 1alpha, 25-dihydroxyvitamin D3 mediated osteoclastogenesis in dental follicle cells. *Scientific Reports, 6*, 24225.

Wise, G. E. (2009). Cellular and molecular basis of tooth eruption. *Orthodontics & Craniofacial Research, 12*(2), 67–73.

Wise, G. E., & King, G. J. (2008). Mechanisms of tooth eruption and orthodontic tooth movement. *Journal of Dental Research, 87*(5), 414–434.

Wise, G. E., Yao, S., & Henk, W. G. (2007). Bone formation as a potential motive force of tooth eruption in the rat molar. *Clinical Anatomy, 20*(6), 632–639.

Wise, G. E., Yao, S., Odgren, P. R., & Pan, F. (2005). CSF-1 regulation of osteoclastogenesis for tooth eruption. *Journal of Dental Research, 84*(9), 837–841.

Xu, H., Snider, T. N., Wimer, H. F., Yamada, S. S., Yang, T., Holmbeck, K., & Foster, B. L. (2016). Multiple essential MT1-MMP functions in tooth root formation, dentinogenesis, and tooth eruption. *Matrix Biology, 52-54*, 266–283.

Xu, J., Li, Z., Hou, Y., & Fang, W. (2015). Potential mechanisms underlying the Runx2 induced osteogenesis of bone marrow mesenchymal stem cells. *American Journal of Translational Research, 7*(12), 2527–2535.

Yan, W. J., Zhang, C. Y., Yang, X., Liu, Z. N., Wang, X. Z., Sun, X. Y., ... Zheng, S. G. (2015). Abnormal differentiation of dental pulp cells in cleidocranial dysplasia.

Journal of Dental Research, 94(4), 577–583.

Yoda, S., Suda, N., Kitahara, Y., Komori, T., & Ohyama, K. (2004). Delayed tooth eruption and suppressed osteoclast number in the eruption pathway of heterozygous Runx2/Cbfa1 knockout mice. *Archives of Oral Biology, 49*(6), 435–442.

Zhang, C., Zheng, S., Wang, Y., Zhao, Y., Zhu, J., & Ge, L. (2010). Mutational analysis of RUNX2 gene in Chinese patients with cleidocranial dysplasia. *Mutagenesis, 25*(6), 589–594.

Zhang, C. Y., Zheng, S. G., Wang, Y. X., Zhu, J. X., Zhu, X., Zhao, Y. M., & Ge, L. H. (2009). Novel RUNX2 mutations in Chinese individuals with cleidocranial dysplasia. *Journal of Dental Research, 88*(9), 861–866.

Zhang, X., Liu, Y., Wang, X., Sun, X., Zhang, C., & Zheng, S. (2017). Analysis of novel RUNX2 mutations in Chinese patients with cleidocranial dysplasia. *PloS One, 12*(7), e0181653.